Positive Polynomial Constraints for POD-based Model Predictive Controllers

Oscar Mauricio Agudelo, Michel Baes, Jairo José Espinosa, *Senior Member, IEEE*, Moritz Diehl, and Bart De Moor, *Fellow, IEEE*

***Abstract*—This paper presents an application of positive polynomials to the reduction of the number of temperature constraints of a proper orthogonal decomposition (POD)-based predictive controller for a non-isothermal tubular reactor. The objective of the controller is to maintain the reactor at a desired operating condition in spite of disturbances in the feed flow, while keeping the maximum temperature low enough to avoid the formation of undesired byproducts. The controller is based on a model derived by means of POD, which reduces the high dimensionality of the discretized system used to approximate the partial differential equations that model the reactor. However, POD does not lead to a reduction in the number of temperature constraints which is typically very large. If we use univariate polynomials to approximate part of the basis vectors derived with the POD technique, it is possible to apply the theory of positive polynomials to find good approximations of the temperature constraints by linear matrix inequalities and to get a reduction in their number. This is the approach that is followed in this paper. The simulation results show that the predictive controller presented a good behavior and that it dealt with the temperature constraints very well.**

***Index Terms*—Distributed parameter systems, model reduction, polynomial approximation, predictive control.**

I. Introduction

TUBULAR reactors are distributed parameter systems that typically are modeled by coupled non-linear partial differential equations (PDEs) which are derived from mass and energy balance principles. A way of addressing the control of these systems is by approximating the PDEs by a large number of ordinary differential equations (ODEs). Afterwards, given the high-dimensionality of the resulting systems, reduced order models are derived to make controller design possible. In this paper, such reduced order models are found by means of proper orthogonal decomposition (POD) and Galerkin projection. The advantage of applying these techniques is the incorporation of simulated or experimental data as well as the existing physical relationships from the original model [1].

In [2], a POD-based Predictive controller is proposed for controlling the temperature and concentration profiles of a non-isothermal tubular chemical reactor. The control goal is to reject the disturbances that affect the process, that is, the changes in the temperature and concentration of the feed flow. One important constraint of the system is that the temperature inside the reactor must be below a given value in order to prevent undesirable side reactions. Under typical disturbances, the controller proposed in [2] performs very well, and the temperature constraint is not violated despite the fact that the predictive controller does not incorporate this constraint in its formulation. However, if larger disturbances are applied, temporary violations of this constraint are observed.

In this paper we start by presenting an extension of the controller proposed in [2]. This new controller takes into account the temperature constraint of the reactor and uses a slack variable approach with ℓ_∞-norm and time-dependent weights for handling the infeasibilities that can emerge [3]. Although POD can find a reduced order model for the reactor, it does not reduce the number of temperature constraints, and therefore the controller has to deal with a very large number of them.

In this paper, we propose a method for approximating the temperature constraints by means of the theory of positive polynomials. This approximation leads to a reduction in the number of constraints by replacing many inequalities by a few linear matrix inequalities (LMIs). This is the main contribution of this paper.

Based on the polynomial approximations of the temperature constraints, a second POD-based MPC controller is proposed. This new controller also incorporates the mechanism for handling infeasibilities of the first predictive controller.

This paper is organized as follows. Section II presents a description of the process. In Section III, the procedure for deriving the reduced order model of the reactor by means of POD and the Galerkin projection is discussed. Section IV describes a POD-based MPC control system that deals with a very large number of temperature constraints. In Section V, our new method for approximating the temperature constraints is described and a new MPC controller is presented. Section VI shows the simulation results of the control schemes presented

Manuscript received June 30, 2007; revised March 10, 2008. Current version published May 13, 2009. This work was supported by the Research Council KUL: CoE EF/05/006 Optimization in Engineering (OPTEC), GOA AMBioRICS, IOF-SCORES4CHEM, several PhD/Postdoc & Fellow Grants; Flemish Government: FWO: PhD/Postdoc Grants, projects G.0452.04 (new quantum algorithms), G.0499.04 (Statistics), G.0211.05 (Nonlinear), G.0226.06 (cooperative systems and optimization), G.0321.06 (Tensors), G.0302.07 (SVM/Kernel, research communities (ICCoS, ANMMM, MLDM); IWT: PhD Grants, McKnow-E, Eureka-Flite2 Belgian Federal Science Policy Office: IUAP P6/04 (Dynamical systems, control and optimization, 2007–2011); EU: ERNS. Recommended by Guest Editors G. Chesi and D. Henrion.

O. M. Agudelo is with the Department of Electrical Engineering (ESAT), Research Group SCD-SISTA, Katholieke Universiteit Leuven, Heverlee B-3001, Belgium and also with the Department of Automation and Electronics, Universidad Autónoma de Occidente,Calle 25 No. 115-85, Cali, Colombia (e-mail: mauricio.agudelo@esat.kuleuven.be).

M. Baes, B. De Moor, and M. Diehl are with the Department of Electrical Engineering (ESAT), Research Group SCD-SISTA, Katholieke Universiteit Leuven, Heverlee B-3001, Belgium (e-mail: michel.baes@esat.kuleuven.be; moritz.diehl@esat.kuleuven.be; bart.demoor@esat.kuleuven.be).

J. J. Espinosa is with the Facultad de Minas, Universidad Nacional de Colombia, Carrera 80 No. 65-223, Medellín, Colombia (e-mail: jairo.espinosa@ieee.org).

Digital Object Identifier 10.1109/TAC.2009.2017136

0018-9286/$25.00 © 2009 IEEE

Authorized licensed use limited to: Katholieke Universiteit Leuven. Downloaded on September 1, 2009 at 08:41 from IEEE Xplore. Restrictions apply.

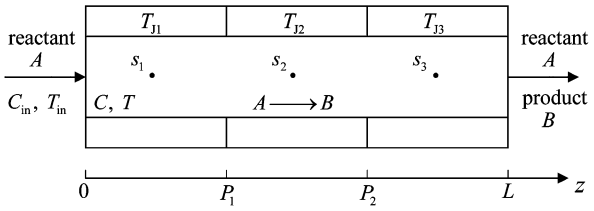

Fig. 1. Tubular reactor with three cooling/heating jackets.

in the previous two sections. Finally Section VII summarizes and concludes the paper.

II. Description of the Process

The process to be controlled is a non-isothermal tubular reactor where a single, first order, irreversible, exothermic reaction takes place ($A \rightarrow B$). The reactor is surrounded by 3 cooling/heating jackets as shown in Fig. 1. The temperature of the jacket fluids (T_{J1}, T_{J2} and T_{J3}) can be manipulated independently in order to control the concentration and temperature profiles in the reactor. In addition, the reactor is characterized by a plug-flow behavior because the diffusion and dispersion phenomena are not taken into account. Under these assumptions, the mathematical model of the tubular chemical reactor consists of the following system of coupled non-linear PDEs:

$$\begin{aligned}\frac{\partial C}{\partial t} &= -v\frac{\partial C}{\partial z} - k_0 C e^{-(E/(RT))} \\ \frac{\partial T}{\partial t} &= -v\frac{\partial T}{\partial z} + G_r C e^{-(E/(RT))} + H_r(T_w - T) \\ G_r &= \frac{-\Delta H k_0}{\rho C_p}, \quad H_r = \frac{4h}{2r_s \rho C_p}\end{aligned} \tag{1}$$

with the following boundary conditions: $C = C_{\text{in}}$ at $z = 0$ and $T = T_{\text{in}}$ at $z = 0$.

Here, $C(z,t)$ is the reactant concentration in [mol/l], $T(z,t)$ is the reactant temperature in [K], v is the fluid superficial velocity in [m/s], $(-\Delta H)$ is the heat of the reaction in [cal/mol], ρ and C_p are the density in [kg/l] and the specific heat in [cal/kg/K] of the mix, respectively, k_0 is the kinetic constant in [1/s], E is the activation energy in [cal/mol], R is the ideal gas constant in [cal/mol/K], h is the heat transfer coefficient in $[\text{cal}/\text{s}/\text{m}^2/\text{K}]$, r_s is the reactor radius in [m], L is the reactor length in [m], C_{in} and T_{in} are the concentration in [mol/l] and the temperature in [K] of the feed flow, z is the axial coordinate in [m], t is the time in [s] and $T_w(z,t)$ is the reactor wall temperature in [K] defined as follows (see Fig. 1):

$$T_w = \begin{cases} T_{J1}, & 0 \le z < P_1 \\ T_{J2}, & P_1 \le z < P_2 \\ T_{J3}, & P_2 \le z \le L. \end{cases}$$

The parameters of the reactor model are taken from [4], which were inspired by the values given in [5]. These values are: $v = 0.1\ \text{m}\cdot\text{s}^{-1}$, $L = 1\ \text{m}$, $k_0 = 10^6 \cdot \text{s}^{-1}$, $E = 11250\ \text{cal}\cdot\text{mol}^{-1}$, $R = 1.986\ \text{cal}\cdot\text{mol}^{-1}\cdot\text{K}^{-1}$, $C_{\text{in}} = 0.02\ \text{mol}\cdot\text{l}^{-1}$, $T_{\text{in}} = 340\ \text{K}$, $G_r = 4.25 \cdot 10^9\ \text{l}\cdot\text{K}\cdot\text{mol}^{-1}\cdot\text{s}^{-1}$, and $H_r = 0.2\ \text{s}^{-1}$.

The temperature of the jacket sections T_{J1}, T_{J2} and T_{J3} must be between 280 K and 400 K. In addition, the temperature inside the reactor must be below 400 K in order to avoid the formation of side products. The kind of disturbances that affects the reactor are principally the variations in the temperature and concentration of the feed flow. Typically, such variations are in the range of ± 10 K for the temperature and $\pm 5\%$ of the nominal value for the concentration. In this system, only the temperature of the feed flow is measured directly. In addition, the reactor has a temperature sensor at the output and 3 temperature sensors (s_1, s_2 and s_3) distributed in its interior as shown in Fig. 1.

A. Operating Profiles

In [2], an optimization algorithm (a kind of SQP) is proposed for deriving the optimal operating profiles of the tubular reactor described by (1). The algorithm minimizes a given cost function subject to the steady-state equations of the reactor and the input and output constraints of the system. The steady-state model of the reactor is given by the following ODEs:

$$\begin{aligned}\frac{dC}{dz} &= -\frac{k_0}{v} C e^{-(E/(RT))} \\ \frac{dT}{dz} &= \frac{G_r}{v} C e^{-(E/(RT))} + \frac{H_r}{v}(T_w - T)\end{aligned} \tag{2}$$

with $T = T_{\text{in}}$ at $z = 0$ and $C = C_{\text{in}}$ at $z = 0$, and the discrete version of (2) can be found by replacing the spatial derivatives by forward difference approximations as follows:

$$\begin{aligned}\bar{C}_{i+1} &= \bar{C}_i - \frac{k_0 \Delta z}{v} \bar{C}_i e^{-(E/(RT_f \bar{T}_i))} \\ \bar{T}_{i+1} &= \bar{T}_i \left[1 - \frac{H_r \Delta z}{v}\right] + \\ &\quad + \left[\frac{G_r \Delta z C_f}{v T_f}\right] \bar{C}_i e^{-(E/(RT_f \bar{T}_i))} + \left[\frac{H_r \Delta z}{v}\right] \bar{T}_{w,i} \\ \bar{T}_0 &= \frac{T_{\text{in}}}{T_f}, \quad \bar{C}_0 = \frac{C_{\text{in}}}{C_f} \\ &\text{for } i = 1, 2, \ldots, N = 300\end{aligned} \tag{3}$$

where T_f and C_f are normalization factors, $\bar{C}_i = C_i/C_f$ and $\bar{T}_i = T_i/T_f$ are the normalized concentration and temperature of the ith section, $\bar{T}_{w,i} = T_{w,i}/T_f$ is the normalized reactor wall temperature of the ith section, N is the number of sections in which the reactor is divided, and Δz is the length of each section. The optimization problem that is solved in [2] for deriving the operating profiles is defined as

$$\min_{\bar{T}_{J1}, \bar{T}_{J2}, \bar{T}_{J3}} w\left(\bar{C}_r - \bar{C}_N\right)^2 + (1-w)\frac{1}{N}\sum_{i=1}^{N}\left(\bar{T}_{r,i} - \bar{T}_i\right)^2 \tag{4}$$

subject to

$$\begin{aligned}&\text{steady-state model given by (3)} \\ &\frac{T_{J_{\min}}}{T_f} \le \bar{T}_{J1}, \bar{T}_{J2}, \bar{T}_{J3} \le \frac{T_{J_{\max}}}{T_f} \\ &\bar{T}_i \le \frac{T_{\max}}{T_f}, \text{ for } i = 1, 2, \ldots, N = 300\end{aligned}$$

where $\bar{C}_r$ is the normalized desired concentration at the reactor output, $\bar{T}_{r,i}$ is the normalized desired temperature inside the reactor of the ith section, $\bar{C}_N$ is the normalized concentration at the reactor output, w is a trade-off parameter, $T_{J_{\min}}$ and $T_{J_{\max}}$ are the limits of the jackets temperatures, and $T_{\max}$ is the maximum allowed temperature inside the tubular reactor.

Authorized licensed use limited to: Katholieke Universiteit Leuven. Downloaded on September 1, 2009 at 08:41 from IEEE Xplore. Restrictions apply.

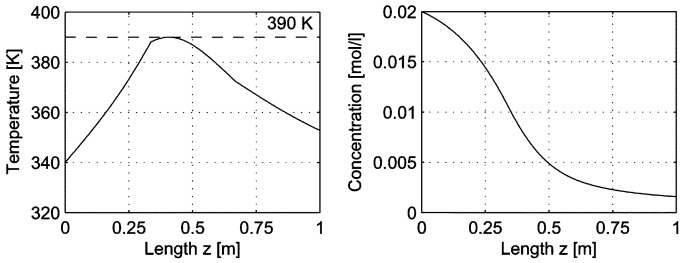

Fig. 2. Steady-state concentration and temperature profiles (operating profiles) when $T_{J1} = 374.6$ K, $T_{J2} = 310.1$ K, and $T_{J3} = 325.2$ K.

The first term of the cost function corresponds to the squared error of the normalized concentration at the reactor output (terminal cost), and the second term is related to the mean squared error of the normalized temperature along the reactor (integral cost). In this problem $\bar{C}_r$ was set to 0, and $\bar{T}_{r,i}$ was selected equal to the normalized temperature of the feeding flow ($\bar{T}_{\text{in}} = (T_{\text{in}}/T_f)$) for $i = 1, 2, \ldots, N$. The trade-off parameter w can take values from 0 to 1. When w goes to 1, the reduction of the reactant concentration at the reactor output becomes more important than the temperature deviations. On the other hand when w goes to 0, the temperature deviations become more important than the concentration at the reactor output and the risk of the formation of hot spots is reduced.

The optimization problem stated by (4) was solved $(w = 0.3)$ by means of the algorithm proposed in [2] (a sort of SQP), and the profiles derived are shown in Fig. 2 together with the corresponding jacket temperatures. The concentration at the reactor output is $1.57 \cdot 10^{-3}$ mol/l, which is 12.7 times smaller than the concentration of the feed flow (0.02 mol/l). Notice that the temperature of the hot spot is 390 K. In the steady-state optimization algorithm, the maximum temperature allowed inside the reactor $T_{\max}$ was set 10 degrees below the actual limit (400 K) in order to give to the feedback controller enough room of maneuverability.

B. Linear Model

As it was done in [2], the linear model of the tubular reactor is obtained by linearizing (1) around the jacket temperatures and the operating profiles presented in Fig. 2. Subsequently, the infinite dimensionality of the resulting linear PDEs is reduced by replacing partial derivatives with respect to space by backward finite difference approximations, leading to the following system of ODEs:

$$\begin{aligned} \dot{\mathbf{x}}(t) &= \mathbf{A}\mathbf{x}(t) + \mathbf{B}\mathbf{u}(t) + \mathbf{F}\mathbf{d}(t) \\ \mathbf{x}(t) &= \left(\bar{C}_1^{\Delta}, \bar{C}_2^{\Delta}, \ldots, \bar{C}_N^{\Delta}, \bar{T}_1^{\Delta}, \bar{T}_2^{\Delta}, \ldots, \bar{T}_N^{\Delta}\right)^T \\ \mathbf{d}(t) &= \left(\bar{C}_{\text{in}}^{\Delta}, \bar{T}_{\text{in}}^{\Delta}\right)^T, \quad \mathbf{u}(t) = \left(\bar{T}_{J1}^{\Delta}, \bar{T}_{J2}^{\Delta}, \bar{T}_{J3}^{\Delta}\right)^T \end{aligned} \tag{5}$$

where C_i^*, T_i^* are the steady state concentration and temperature of the ith section, C_{in}^* and T_{in}^*, are the steady state concentration and temperature of the feed flow, T_{J1}^*, T_{J2}^*, T_{J3}^* are the steady state jacket temperatures, T_f and C_f are normalization factors, $\bar{C}_i^{\Delta} = (C_i - C_i^*)/C_f$, $\bar{T}_i^{\Delta} = (T_i - T_i^*)/T_f$ are the normalized deviations from steady state of the concentration and temperature of the ith section, $\bar{C}_{\text{in}}^{\Delta} = (C_{\text{in}} - C_{\text{in}}^*)/C_f$ and $\bar{T}_{\text{in}}^{\Delta} = (T_{\text{in}} - T_{\text{in}}^*)/T_f$ are the normalized deviations from steady state of the concentration and temperature of the feed flow, $\bar{T}_{J1}^{\Delta} = (T_{J1} - T_{J1}^*)/T_f$, $\bar{T}_{J2}^{\Delta} = (T_{J2} - T_{J2}^*)/T_f$ and $\bar{T}_{J3}^{\Delta} = (T_{J3} - T_{J3}^*)/T_f$ are the normalized deviations of the jacket temperatures, N is the number of sections in which the reactor is divided, $\mathbf{A}$, $\mathbf{B}$ and $\mathbf{F}$ are the matrices describing the system, $\mathbf{x}(t)$ is the state vector, $\mathbf{u}(t)$ is the vector of the inputs, and $\mathbf{d}(t)$ is the vector of the disturbances.

Since the spatial domain of the reactor is divided into $N = 300$ sections, the number of states of (5) is equal to 600. This large number of states makes the design and implementation of feedback controllers for the reactor difficult. Consequently, it is necessary to find a reduced order model. In this study such a reduced order model is found using Proper Orthogonal Decomposition (POD) and Galerkin projection [6]. A detailed explanation of the procedure is given in [2]. Nevertheless, in order to make this paper self contained, this procedure is presented briefly in Section III.

III. Model Reduction by Means of POD

In proper orthogonal decomposition (POD) [7]–[15], we start by observing that $\mathbf{x}(t) \in \Re^{2N}$ can be expanded as a sum of orthonormal basis vectors

$$\mathbf{x}(t) = \sum_{j=1}^{2N} a_j(t)\boldsymbol{\varphi}_j \tag{6}$$

where $\boldsymbol{\varphi}_j \in \Re^{2N}\ \forall j = 1, \ldots, 2N$ is a set of orthonormal basis vectors (POD basis vectors or POD basis functions) in the discretized spatial domain, and $a_j(t) \in \Re\ \forall j = 1, \ldots, 2N$ are the time-varying coefficients, or POD coefficients, associated to each basis vector. These POD basis vectors are ordered according to their relevance to $\mathbf{x}(t)$.

The main dynamics of the system can be represented using the first n most relevant basis vectors, since $\boldsymbol{\varphi}_1, \boldsymbol{\varphi}_2, \ldots, \boldsymbol{\varphi}_n$ condensates the main spatial correlations. An nth order approximation of (6) is then given by means of the truncated sequence

$$\mathbf{x}_n(t) = \sum_{j=1}^{n} a_j(t)\boldsymbol{\varphi}_j, \quad n \ll 2N. \tag{7}$$

An approximate (reduced order) model of $\mathbf{x}(t)$ can be derived by building a model for the first n time-varying coefficients. This is the essence of model reduction by POD. The POD basis vectors are determined from simulation or experimental data of the process. The dynamic model for the first n time-varying coefficients can be found by means of Galerkin projection [6], [15]–[19] or using subspace identification techniques [20]–[22].

In Sections III-A–D, we describe the steps followed for deriving the reduced order model of (5).

A. Generation of the Snapshot Matrix

We have constructed a snapshop matrix $\mathbf{X}_{\text{snap}} \in \Re^{600 \times 1500}$ from the system response when independent step changes were made in the input $\mathbf{u}(t)$ and perturbation $\mathbf{d}(t)$ signals of the linear model (5)

$$\mathbf{X}_{\text{snap}} = (\mathbf{x}(t = \Delta t), \ldots, \mathbf{x}(t = 1500\Delta t)).$$

Authorized licensed use limited to: Katholieke Universiteit Leuven. Downloaded on September 1, 2009 at 08:41 from IEEE Xplore. Restrictions apply.

Along the simulations, 1500 samples were collected. The amplitude of the step changes was chosen in such a way as to produce changes of similar magnitude in the temperature and concentration profiles. This avoids a possible bias in the resulting model.

B. Derivation of the POD Basis Vectors

The POD basis vectors were derived by calculating the singular value decomposition (SVD) of $\mathbf{X}_{\text{snap}}$

$$\mathbf{X}_{\text{snap}} = \mathbf{\Phi}\mathbf{\Sigma}\mathbf{\Psi}^T$$

where $\mathbf{\Phi} \in \Re^{600\times 600}$ and $\mathbf{\Psi} \in \Re^{1500\times 1500}$ are unitary matrices, and $\mathbf{\Sigma} \in \Re^{600\times 1500}$ is a matrix that contains the singular values of $\mathbf{X}_{\text{snap}}$ in a decreasing order on its main diagonal. The columns of $\mathbf{\Phi}$ are the POD basis vectors

$$\mathbf{\Phi} \in \Re^{600\times 600} = (\boldsymbol{\varphi}_1, \boldsymbol{\varphi}_2, \ldots, \boldsymbol{\varphi}_{600}).$$

C. Selection of the Most Relevant POD Basis Vectors

We have performed the selection by checking the singular values of $\mathbf{X}_{\text{snap}}$ (the larger the singular value the more relevant the basis vector is) and the truncation degree P_n of (7), which is defined as follows:

$$P_n = \frac{\sum_{j=1}^{n} \sigma_j^2}{\sum_{j=1}^{2N} \sigma_j^2}; \quad n = 1, \ldots, 2N \tag{8}$$

where σ_j is the jth singular value of $\mathbf{X}_{\text{snap}}$. The number of POD basis elements can be chosen so that the fraction of the first singular values in (8) is large enough to capture most information in the data [6]. An ad-hoc criterion commonly applied is that n has to be determined for $P = 0.99$[23]. In this problem, the first 20 basis vectors were selected. The 20th order approximation of $\mathbf{x}(t)$ is given by

$$\mathbf{x}_{20}(t) = \sum_{j=1}^{20} a_j(t)\boldsymbol{\varphi}_j = \mathbf{\Phi}_{20}\mathbf{a}(t) \tag{9}$$

where $\mathbf{\Phi}_{20} = (\boldsymbol{\varphi}_1, \ldots, \boldsymbol{\varphi}_{20})$ and $\mathbf{a}(t) = (a_1(t), \ldots, a_{20}(t))^T$.

D. Construction of the Model for the First $n = 20$ POD Coefficients

In order to derive a dynamic model for the POD coefficients, we have used the Galerkin projection. If we define a residual function $R(\mathbf{x}, \dot{\mathbf{x}})$ for (5) as follows:

$$R(\mathbf{x}, \dot{\mathbf{x}}) = \dot{\mathbf{x}}(t) - \mathbf{A}\mathbf{x}(t) - \mathbf{B}\mathbf{u}(t) - \mathbf{F}\mathbf{d}(t) \tag{10}$$

and we replace $\mathbf{x}(t)$ by its nth order approximation $\mathbf{x}_n(t)$ in (10), the projection of $R(\mathbf{x}_n, \dot{\mathbf{x}}_n)$ on the space spanned by the basis vectors $\mathbf{\Phi}_n$ shall vanish. That is

$$\langle R(\mathbf{x}_n, \dot{\mathbf{x}}_n), \boldsymbol{\varphi}_j \rangle = 0; \quad j = 1, \ldots, n \tag{11}$$

where $\langle \cdot, \cdot \rangle$ denotes the Euclidean inner product. Replacing $\mathbf{x}(t)$ by its nth order approximation $\mathbf{x}_n(t) = \mathbf{\Phi}_n\mathbf{a}(t)$ in (5), and applying the inner product criterion (11) to the resulting equation we have

$$\begin{aligned}\mathbf{\Phi}_n^T\mathbf{\Phi}_n\dot{\mathbf{a}}(t) &= \mathbf{\Phi}_n^T\mathbf{A}\mathbf{\Phi}_n\mathbf{a}(t) + \mathbf{\Phi}_n^T\mathbf{B}\mathbf{u}(t) + \mathbf{\Phi}_n^T\mathbf{F}\mathbf{d}(t)\\ \dot{\mathbf{a}}(t) &= \mathbf{\Phi}_n^T\mathbf{A}\mathbf{\Phi}_n\mathbf{a}(t) + \mathbf{\Phi}_n^T\mathbf{B}\mathbf{u}(t) + \mathbf{\Phi}_n^T\mathbf{F}\mathbf{d}(t).\end{aligned}$$

The reduced order model of the reactor is then given by

$$\begin{aligned}\dot{\mathbf{a}}(t) &= \mathbf{A}_r\mathbf{a}(t) + \mathbf{B}_r\mathbf{u}(t) + \mathbf{F}_r\mathbf{d}(t)\\ \mathbf{x}_n(t) &= \mathbf{\Phi}_n\mathbf{a}(t)\end{aligned} \tag{12}$$

where $\mathbf{A}_r = \mathbf{\Phi}_n^T\mathbf{A}\mathbf{\Phi}_n$, $\mathbf{B}_r = \mathbf{\Phi}_n^T\mathbf{B}$ and $\mathbf{F}_r = \mathbf{\Phi}_n^T\mathbf{F}$. The initial condition for $\mathbf{a}(t)$ reads as $\mathbf{a}(0) = \mathbf{0}$.

Finally, the discrete-time version of (12) that is used by the predictive controllers, was obtained using the bilinear transformation [24] with a sampling time of 0.2 s

$$\begin{aligned}\mathbf{a}(k+1) &= \tilde{\mathbf{A}}\mathbf{a}(k) + \tilde{\mathbf{B}}\mathbf{u}(k) + \tilde{\mathbf{F}}\mathbf{d}(k)\\ \mathbf{x}_n(k) &= \mathbf{\Phi}_n\mathbf{a}(k)\end{aligned} \tag{13}$$

where $\tilde{\mathbf{A}}$, $\tilde{\mathbf{B}}$ and $\tilde{\mathbf{F}}$ are the matrices describing the new system. The sampling time was chosen by dividing the smallest time constant of the system (12) by 10.

IV. Predictive Control Scheme

The control objective is to reject the disturbances that affect the reactor, that is the changes in the temperature and concentration of the feed flow. In addition, the control actions must satisfy the input constraints of the process, and the control system should keep the temperature inside the reactor below 400 K.

In [2], a POD-based MPC control scheme is proposed for controlling the reactor. Although this controller performs well in the tests presented in [2] (the reactor is subject to typical disturbances as described in Section II), it does not incorporate the temperature constraint of the reactor on its formulation. Therefore, when larger disturbances than the typical ones are applied, temporary violations of the temperature constraint will be observed. In this section we present an extension of the control scheme described in [2], which takes into account the temperature constraint of the reactor.

The control of the temperature and concentration profiles is achieved indirectly by controlling the POD coefficients. The references $(\mathbf{a}_{\text{ref}})$ of these POD coefficients can be calculated by

$$\mathbf{a}_{\text{ref}} = \mathbf{\Phi}_n^T\mathbf{x}_{\text{ref}} \tag{14}$$

where $\mathbf{x}_{\text{ref}}$ is the reference of the vector $\mathbf{x}(t)$ and is equal to $\mathbf{0}$ since the control system has to keep the reactor operating around the profiles shown in Fig. 2.

Since in this MPC formulation the temperature constraint along the reactor is taken into account, it is necessary to define a mechanism for handling the infeasibilities that can emerge due to the differences between the process and the model used by the MPC, the magnitude of the disturbances, the saturation of the actuators, etc. A way of dealing with these infeasibilities is by

Authorized licensed use limited to: Katholieke Universiteit Leuven. Downloaded on September 1, 2009 at 08:41 from IEEE Xplore. Restrictions apply.

softening the temperature constraint through a *slack variable* approach. A soft constraint formulation avoids infeasibility problems by allowing violations in the temperature constraint, but at the same time it tries to minimize such violations by penalizing them in the objective function. In this paper a slack variable approach with ℓ_∞-norm and time-dependent weights is used [3], [25]. The MPC controller is formulated as follows:

$$\min_{a,\Delta u,d,u,\varepsilon} J = \sum_{k=1}^{N_p} \|\mathbf{a}_{\text{ref}} - \mathbf{a}(k)\|^2_{\mathbf{Q}} + \sum_{k=0}^{N_c-1} \|\Delta\mathbf{u}(k)\|^2_{\mathbf{R}} + P_Q\varepsilon^2 + P_L\varepsilon \quad (15a)$$

subject to

$$\begin{aligned}
\mathbf{a}(k+1) &= \tilde{\mathbf{A}}\mathbf{a}(k) + \tilde{\mathbf{B}}\mathbf{u}(k) + \tilde{\mathbf{F}}\mathbf{d}(k), \quad k = 0,\ldots,N_p-1\\
\mathbf{d}(k+1) &= \mathbf{d}(k), \quad k = 0,\ldots,N_p-1\\
\mathbf{u}(k+1) &= \mathbf{u}(k) + \Delta\mathbf{u}(k+1), \quad k = -1,\ldots,N_c-2\\
\mathbf{u}(k+1) &= \mathbf{u}(k), \quad k = N_c-1,\ldots,N_p-1\\
\mathbf{u}_{\min} &\le \mathbf{u}(k) \le \mathbf{u}_{\max} \qquad (15b)\\
\bar{\mathbf{T}}^{\Delta}(k) &= \mathbf{\Phi}_T\mathbf{a}(k) \le \bar{\mathbf{T}}^{\Delta_{\max}} + \mathbf{1}\cdot\eta(k)\varepsilon, \qquad (15c)\\
\varepsilon &\ge 0, \quad \text{for } k = 1,\ldots,N_p \qquad (15d)
\end{aligned}$$

where $\mathbf{Q}$ and $\mathbf{R}$ are weighting matrices ($\mathbf{Q} \succeq 0, \mathbf{R} \succeq 0$), $\|\mathbf{v}\|^2_{\mathbf{Q}}$ denotes $\mathbf{v}^T\mathbf{Q}\mathbf{v}$, N_p is the prediction horizon, N_c is the control horizon, $\mathbf{u}_{\min}$ and $\mathbf{u}_{\max}$ are the lower and upper bounds (these hard constraints are necessary due to physical limitations of the actuators) of $\mathbf{u}(k)$, $\bar{\mathbf{T}}^{\Delta}(k) = \mathbf{\Phi}_T\mathbf{a}(k)$ is a vector which contains the normalized deviations of the temperature profile, $\mathbf{\Phi}_T$ is the lower part (the last $N = 300$ rows) of the matrix $\mathbf{\Phi}_n = \left(\mathbf{\Phi}_C^T, \mathbf{\Phi}_T^T\right)^T$ that is associated to the temperature profile, $\bar{\mathbf{T}}^{\Delta_{\max}} = (400\,\text{K}\cdot\mathbf{1} - \mathbf{T}^*)/T_f$ is a vector that contains the maximal allowed temperature for each point of the reactor, ε is the slack variable (a scalar quantity), P_Q and P_L are weighting factors ($P_Q > 0$, $P_L > 0$), $\mathbf{1} \in \Re^{300}$ is a vector of 1's and $\eta(k) = 1/r^{k-1}$, is a time-dependent weight ($r > 1$).

In this formulation the maximum violation of the temperature constraint along the reactor and the prediction horizon is penalized by means of the term $P_Q\varepsilon^2 + P_L^T\varepsilon$. A sufficiently large P_L will ensure that the constraints are enforced as exact soft constraints, that is, that constraint violations will only occur when there is not feasible solution of the original problem [3]. The quadratic term $P_Q\varepsilon^2$ is used as an additional tuning parameter and it also leads to a well-posed quadratic program (positive definite Hessian) [26].

The time-dependent weight $\eta(k)$ penalizes future predicted constraint violations increasingly, avoiding long-lasting constraint violations [3].

Since the state vector $\mathbf{a}(k)$ is unknown and the changes in the concentration of the feed flow $d_1(k) = \bar{C}^{\Delta}_{\text{in}}(k)$ are not measured directly, they are estimated by means of an observer (in this case a Kalman Filter) with the following formulation:

$$\begin{pmatrix} \hat{\mathbf{a}}(k+1) \\ \hat{d}_1(k+1) \end{pmatrix} = \begin{pmatrix} \tilde{\mathbf{A}} & \tilde{\mathbf{F}}_C \\ \mathbf{0} & 1 \end{pmatrix} \begin{pmatrix} \hat{\mathbf{a}}(k) \\ \hat{d}_1(k) \end{pmatrix} + \begin{pmatrix} \tilde{\mathbf{B}} \\ \mathbf{0} \end{pmatrix} \mathbf{u}(k) + \begin{pmatrix} \tilde{\mathbf{F}}_T \\ 0 \end{pmatrix} d_2(k) + \begin{pmatrix} \mathbf{L}_a \\ \mathbf{L}_d \end{pmatrix} (\mathbf{y}(k) - \hat{\mathbf{y}}(k)) \quad (16a)$$

$$\hat{\mathbf{y}}(k) = \mathbf{C}_s\hat{\mathbf{x}}_n(k) = \mathbf{C}_s\mathbf{\Phi}_n\hat{\mathbf{a}}(k) \quad (16b)$$

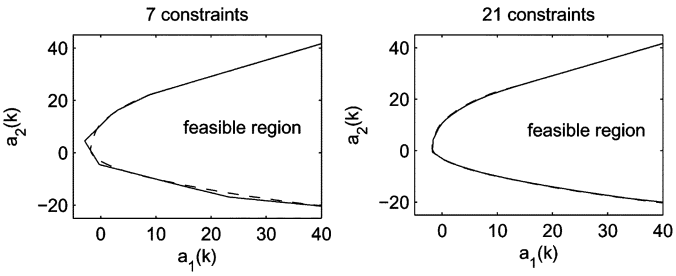

Fig. 3. Feasible regions delimited by the temperature constraints of a second order POD model. Dashed Line—Full set of constraints. Solid Line—Reduced set of constraints.

where $\hat{\mathbf{a}}(k)$ is the estimated vector of the POD coefficients, $\hat{d}_1(k)$ is the estimation of $\bar{C}^{\Delta}_{\text{in}}(k)$, $d_2(k)$ is the normalized temperature deviation of the feed flow $\bar{T}^{\Delta}_{\text{in}}(k)$, $\mathbf{y}(k) \in \Re^4$ is a vector which contains the four temperature measurements (normalized deviations) along the reactor, $\hat{\mathbf{y}}(k)$ is the estimate of $\mathbf{y}(k)$, $\mathbf{L}_a$ and $\mathbf{L}_d$ are the submatrices of the observer gain (Kalman gain), $\tilde{\mathbf{F}}_C$ and $\tilde{\mathbf{F}}_T$ are the column vectors of $\tilde{\mathbf{F}} = (\tilde{\mathbf{F}}_C, \tilde{\mathbf{F}}_T)$ and $\mathbf{C}_s$ is a selection matrix which selects the measured temperatures from the vector $\mathbf{x}_n(k)$.

The control horizon N_c was set to 10 samples and the prediction horizon N_p was selected according to the following criterion: "Prediction Horizon = Control Horizon + Largest Settling Time = 80 samples". $\mathbf{u}_{\min}$ and $\mathbf{u}_{\max}$ were selected according to the input constraints of the process and the operating temperatures of the jackets. The other parameters were selected as follows: $r = 1.2$, $P_L = 10^4$, $P_Q = 10^4$, $\mathbf{Q} = \mathbf{I}_{20\times20}$ and $\mathbf{R} = 110\cdot\mathbf{I}_{3\times3}$.

The optimization problem (15) that is solved by the MPC controller is a quadratic programming (QP) problem which has $N\times N_p = 300\times80 = 24000$ temperature constraints. Although the POD technique has reduced the number of state variables of (5), the number of temperature constraints is still very large. A very intuitive and simple way of reducing the number of constraints is by choosing properly only some of them [27]. In spite of the fact that the POD model of the reactor has 20 states, in Fig. 3 a second order POD model is used for visualizing the feasible regions delimited by the temperature constraints. Notice that with seven constraints we have a fair approximation of the original feasible region (300 constraints). But with 21 temperature constraints, the feasible region delimited by 300 constraints is approximated very accurately. Note however that, with this approach, we do not have any command on the temperature between the discretization points.

In this paper, we present an interesting new approach which uses the positive polynomials theory to tackle the problem. Other ways to tackle it are also possible and might be efficient, like for example the method mentioned previously. Future work will show which technique works best for which kind of applications. In the approach discussed in this manuscript, the large number of linear inequalities is replaced by a few LMIs while maintaining a control of the temperature at every point of the reactor. In Section V we present the details of this technique.

Authorized licensed use limited to: Katholieke Universiteit Leuven. Downloaded on September 1, 2009 at 08:41 from IEEE Xplore. Restrictions apply.

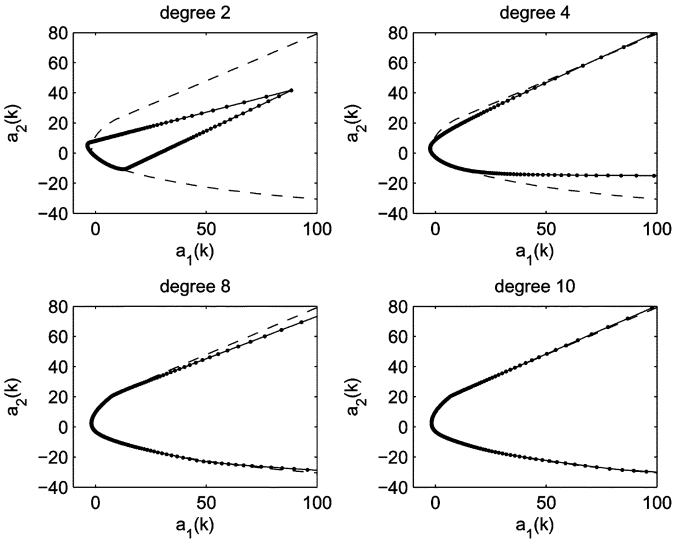

Fig. 4. Feasible regions delimited by the temperature constraints of a second order POD model. Dashed Line—Original temperature constraints. Solid Line—Polynomial Approximations of different degree given by (19). Solid Line with dots—Polynomial Approximations of different degree given by (22).

V. Approximation of the Temperature Constraints By Means of Positive Polynomials

Similarly to the previous section, a second order POD model is used to illustrate and explain the main idea of this positive polynomial approach. Fig. 4 shows in dashed line the feasible region delimited by the temperature constraints

$$\mathbf{\Phi}_T \mathbf{a}(k) \leq \bar{\mathbf{T}}^{\Delta_{\max}} \tag{17}$$

of a second order POD model.

As it was mentioned before, $\mathbf{\Phi}_T \in \Re^{300\times 20}$ is the lower part of the matrix $\mathbf{\Phi}_n = \left(\mathbf{\Phi}_C^T, \mathbf{\Phi}_T^T\right)^T$, therefore each column of $\mathbf{\Phi}_T$ corresponds to the part of the basis vectors $\boldsymbol{\varphi}_j \ \forall j = 1,\ldots,20$ that is associated to the temperature profile. That is

$$\mathbf{\Phi}_T = (\tilde{\boldsymbol{\varphi}}_1, \tilde{\boldsymbol{\varphi}}_2, \ldots, \tilde{\boldsymbol{\varphi}}_j, \ldots, \tilde{\boldsymbol{\varphi}}_{20})$$

where $\tilde{\boldsymbol{\varphi}}_j \in \Re^{300}$ for $j = 1,\ldots,20$.

By taking advantage of the smoothness of the most relevant columns of $\mathbf{\Phi}_T$, we can find polynomial approximations $P_j(z)$ of the vectors $\tilde{\boldsymbol{\varphi}}_j \ \forall j = 1,\ldots,20$ by means of a least squares regression. These approximations would satisfy

$$P_j(z_i) \approx \tilde{\boldsymbol{\varphi}}_{ij} \quad \forall\, j = 1,\ldots,n = 20 \tag{18a}$$

$$P_{\max}(z_i) \approx \bar{\mathbf{T}}_i^{\Delta_{\max}} \quad \text{for } i = 1,2,\ldots,N = 300 \tag{18b}$$

where $\tilde{\boldsymbol{\varphi}}_{ij}$ is the ith element of $\tilde{\boldsymbol{\varphi}}_j$ associated to the ith grid point, $\bar{\mathbf{T}}_i^{\Delta_{\max}}$ is the ith element of $\bar{\mathbf{T}}^{\Delta_{\max}}$ associated to the ith grid point, $P_j(z)$ and $P_{\max}(z)$ are univariate real polynomials of degree d that approximate the vectors $\tilde{\boldsymbol{\varphi}}_j$ and $\bar{\mathbf{T}}^{\Delta_{\max}}$ respectively, z is the spatial coordinate and z_i is the value of the spatial coordinate at the ith grid point.

By using (18a) and (18b) we can approximate (17) by

$$\hat{\mathbf{\Phi}}_T \mathbf{a}(k) \leq \hat{\mathbf{T}}^{\Delta_{\max}} \tag{19}$$

$$\hat{\mathbf{\Phi}}_T = \begin{pmatrix} P_1(z_1) & P_2(z_1) & \ldots & P_n(z_1) \\ P_1(z_2) & P_2(z_2) & \ldots & P_n(z_2) \\ \vdots & \vdots & \ddots & \vdots \\ P_1(z_N) & P_2(z_N) & \ldots & P_n(z_N) \end{pmatrix}$$

$$\hat{\mathbf{T}}^{\Delta_{\max}} = \begin{pmatrix} P_{\max}(z_1) \\ P_{\max}(z_2) \\ \vdots \\ P_{\max}(z_N) \end{pmatrix}$$

where $\hat{\mathbf{\Phi}}_T$ and $\hat{\mathbf{T}}^{\Delta_{\max}}$ are the approximations of $\mathbf{\Phi}_T$ and $\bar{\mathbf{T}}^{\Delta_{\max}}$ respectively, $N = 300$ is the number of sections into which the reactor is divided (number of grid points) and $n = 20$ is the number of the selected POD basis vectors.

Fig. 4 shows the feasible regions (in solid line) delimited by (19) for a second order POD model when polynomials of different degree are used. From this Figure, it is clear that polynomials of degree 10 are accurate enough for approximating $\tilde{\boldsymbol{\varphi}}_j \ \forall j = 1,2$ and $\bar{\mathbf{T}}^{\Delta_{\max}}$.

Equation (19) imposes the temperature constraint only on the grid points of the interval $[0,1]$. However, we can impose the condition (19) on every point of the interval $[0,1]$, giving

$$\sum_{j=1}^{n} a_j(k) P_j(z) \leq P_{\max}(z), \quad \forall\, z \in [0,1]$$

which can be rewritten by defining

$$P^{(k)}(z) = P_{\max}(z) - \sum_{j=1}^{n} a_j(k) P_j(z)$$

as follows:

$$P^{(k)}(z) \geq 0, \quad \forall\, z \in [0,1]. \tag{20}$$

The resulting polynomial $P^{(k)}(z)$ of degree d has to be nonnegative, at least in the interval $z \in [0,1]$.

Even though we have now seemingly complicated the problem by replacing many by infinitely many inequalities, this new formulation can efficiently be handled by positive polynomials techniques.

A. Semidefinite Representability of Positive Polynomials on an Interval

A sufficient condition for a multivariate real polynomial to be nonnegative everywhere is whether it can be written as a sum of squared polynomials. We denote this property, as common, by the acronym SOS, for Sum Of Squares. In general, SOS is not equivalent to the nonnegativity of a polynomial. Nevertheless, as a direct consequence of the Fundamental Theorem of Algebra, univariate real polynomials are nonnegative everywhere if and only if they are SOS.

Further, the SOS representability of a polynomial can be expressed as a semidefinite feasibility problem [28], [29], as the following proposition states for univariate polynomials.

Authorized licensed use limited to: Katholieke Universiteit Leuven. Downloaded on September 1, 2009 at 08:41 from IEEE Xplore. Restrictions apply.

Proposition 1: (see [28]) A univariate polynomial $P(z)$ of degree $2d$ is SOS if and only if there exists a $(d+1)\times(d+1)$ positive semidefinite matrix $\mathbf{W}$ such that

$$P(z)=\mathbf{f}(z)^T\mathbf{W}\mathbf{f}(z) \tag{21}$$

where $\mathbf{f}(z)=(1,z,z^2,\ldots,z^d)^T$.

As the SOS representation of a polynomial is generically not unique, the matrix $\mathbf{W}$ can not be uniquely defined.

It is possible to relate the positivity of a real univariate polynomial on a compact interval $[a,b]$ to the positivity of some other polynomial on the whole real line by the following transformation.

Proposition 2: (see [30, Section 4.2, Example 21.b]) A real univariate polynomial p of degree d is nonnegative on the compact interval $[a,b]$ if and only if

$$(1+z^2)^d p\left(a+\frac{(b-a)z^2}{1+z^2}\right)\geq 0,\quad \forall\, z\in\Re.$$

The proof relies on the observation that the conditions:

- the rational function $g(z)=g_n(z)/g_d(z)$ has $[a,b]$ as image;
- the denominator $g_d(z)$ is positive on $z\in\Re$;
- and $p(z)\geq 0$ on $z\in[a,b]$;

are equivalent to $p(g(z))\geq 0$ on $z\in\Re$.

For every $1\leq k\leq N_p$, the condition (20):

$$P^{(k)}(z)=P_{\max}(z)-\sum_{j=1}^{n}a_j(k)P_j(z)\geq 0,\quad \forall\, z\in[0,1]$$

can be converted into

$$\tilde{P}^{(k)}(z)=(1+z^2)^d P^{(k)}\left(\frac{z^2}{1+z^2}\right)\geq 0,\quad \forall\, z\in\Re$$

and, denoting by S_+^{d+1} the set of $(d+1)\times(d+1)$ positive semidefinite matrices, into

$$\begin{aligned}&\text{find } \mathbf{W}^{(k)}\in S_+^{d+1}\\ &\text{such that } \tilde{P}^{(k)}(z)=\mathbf{f}(z)^T\mathbf{W}^{(k)}\mathbf{f}(z).\end{aligned} \tag{22}$$

Observe that the coefficients of $P^{(k)}(z)$, and thus the coefficients of $\tilde{P}^{(k)}(z)$ depend linearly on $a_j(k)\ \forall j=1,\ldots,n$. Therefore, the coefficients of $\mathbf{W}^{(k)}$ are themselves linear functions of $a_j(k)$. Henceforth, the MPC optimization problem with the polynomial approximation of the temperature constraints can be written as a Semidefinite Program (SDP). SDP are a subclass of *self-scaled* optimization problems (see [31]), that can be solved efficiently by Interior-Point Methods, such as the one implemented in the Matlab toolbox Sedumi [32].

Fig. 4 depicts the feasible regions (solid line with dots) delimited by (22) for a second order POD model when polynomials of different degree are used. Notice how this approximation overlaps completely the approximation given by (19) for all the cases. It means that the error in the approximation given by (22) are mainly due to the errors of approximating the columns of $\mathbf{\Phi}_T$ and $\bar{\mathbf{T}}^{\Delta_{\max}}$ by polynomials.

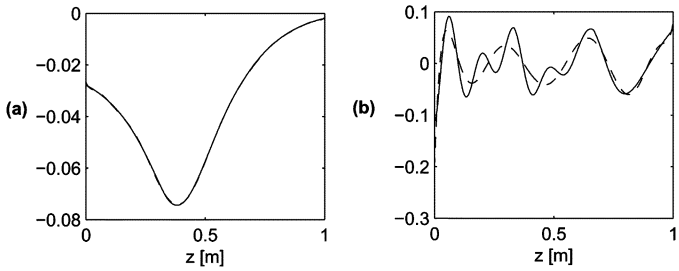

Fig. 5. Polynomial approximations of the vectors (a) $\bar{\boldsymbol{\varphi}}_1$ and (b) $\bar{\boldsymbol{\varphi}}_{20}$. Solid Line—vector. Dashed line—Approximation with a polynomial of degree 12.

For degree 10, the feasible region induced by the polynomial approximation (22) and by the original temperature constraints (17) are almost indistinguishable.

The formulation of the new MPC controller based on polynomial approximations of the temperature constraints would be given by (15), but substituting (15c) by

$$\begin{aligned}\mathbf{W}^{(k)}&\succeq 0\\ \tilde{P}^{(k)}(z)&=\mathbf{f}(z)^T\mathbf{W}^{(k)}\mathbf{f}(z)\end{aligned}$$

with

$$\begin{aligned}\tilde{P}^{(k)}(z)&=(1+z^2)^d P^{(k)}\left(\frac{z^2}{1+z^2}\right)\\ P^{(k)}(z)&=P_{\max}(z)+\eta(k)\varepsilon-\sum_{j=1}^{n}a_j(k)P_j(z).\end{aligned}$$

Here, ε is the slack variable (a scalar quantity) and $\eta(k)=1/r^{k-1}$, is a time-dependent weight $(r>1)$. As it was explained in Section IV, the slack variable ε and the time-dependent weight allow the MPC to deal with possible infeasibilities. Observe that the semidefinite representation of this constraint still yields LMIs, which fall into the scope of interior-point methods for self-scaled programming.

This new MPC has the same tuning parameters as the MPC presented in Section IV. We have set the degree of the polynomials $P_{\max}(z)$ and $P_1(z),P_2(z),\ldots,P_{20}(z)$ to $d=12$. With this selection, the first seven vectors $\tilde{\boldsymbol{\varphi}}_1,\ldots,\tilde{\boldsymbol{\varphi}}_7$ are approximated very well. On the other hand, the last five vectors $\tilde{\boldsymbol{\varphi}}_{15},\ldots,\tilde{\boldsymbol{\varphi}}_{20}$ (the less relevant ones) are approximated very poorly (See Fig. 5). In general, the less important the POD basis function, the more oscillatory it is. If we want to improve the polynomial approximations, we would have to increase d, but this would lead to an increment in the number of constraints.

Unlike the MPC presented in Section IV which deals with 24 000 temperature constraints, this MPC has only $(2d+1)\times N_p=25\times 80=2000$ linear equality constraints and $N_p=80$ LMIs of dimension 13×13 for dealing with the temperature constraint of the reactor. Hence, a large reduction in the number of temperature constraints has been achieved by means of the polynomial approximations.

For the estimation of the state vector $\mathbf{a}(k)$ and the changes in the concentration of the feed flow $d_1(k)=\bar{C}_{\text{in}}^{\Delta}(k)$, this MPC uses the same observer (16) as described in Section IV.

Authorized licensed use limited to: Katholieke Universiteit Leuven. Downloaded on September 1, 2009 at 08:41 from IEEE Xplore. Restrictions apply.

VI. Simulation Results

In order to perform the closed-loop simulations of the control systems described in the previous sections, the nonlinear model of the process given in (1) was discretized in space by replacing the partial derivatives with respect to space by backward difference approximations [4], [33].

In this study, we solve the optimization problem of the MPC controllers by means of *Sedumi*, a Matlab toolbox for optimization over symmetric cones [32]. It is important to remark that all the MPC controllers have been implemented using the condensed form of the MPC formulations presented before. It means that the cost function and constraints of (15) have been expressed in terms of $\Delta\mathbf{u}(k)$ and ε, and the formulation of the MPC controller based on the polynomial approximations has been expressed in terms of $\Delta\mathbf{u}(k)$, ε and the entries of the matrix $\mathbf{W}^{(k)}$.

From now on, the MPC controller (15) will be referred to as MPC-QP and the MPC based on the polynomial approximations (see last part of Section V-A) to as MPC-SDP.

Initially, in order to compare and evaluate the performance of the MPC controllers, we carried out the tests proposed in [2]:

- Test 1: the temperature and concentration of the feed flow are increased by 10 K and 10^{-3} mol/l, respectively.
- Test 2: the temperature and concentration of the feed flow are decreased by 10 K and 10^{-3} mol/l, respectively.

The simulation results of MPC-QP and MPC-SDP were quite similar to the ones shown in [2], where a POD-based MPC controller without temperature constraints is presented. The formulation of this controller is given by (15) after eliminating the (15c), (15d) and the term $P_Q\varepsilon^2 + P_L\varepsilon$ in the cost function. This controller with No Temperature Constraints will be referred to as MPC-NTC.

Along Tests 1 and 2, the MPC-QP, MPC-SDP and MPC-NTC controllers kept the reactor working around the nominal operating profiles, there were no violations of the temperature constraint, the concentration in steady state at the reactor outlet was kept quite close to its nominal value, and the control actions were all the time within the allowed bounds.

The similarities in the results are due to the fact that the control systems were not operating close to the temperature constraints, and therefore during the tests, these constraints are not active in the MPC-QP and MPC-SDP controllers. So, in order to evaluate the ability of MPC-QP and MPC-SDP to deal with the temperature constraints, we propose this new test:

- Test 3: the temperature and concentration of the feed flow are increased by 24 K and $3\cdot10^{-3}$ mol/l, respectively. These disturbances are large in comparison with the typical ones.

Observe that under this test, the tubular reactor operates far from the operating profiles shown in Fig. 2, and therefore the differences between the nonlinear model of the process and the linear POD model used by the controllers are considerable. Figs. 6 and 7 present the simulation results of Test 3.

Notice that in Fig. 6 for all the cases, the steady state profiles of the reactor are overlapping.

In Fig. 7 we can observe that for the case of the MPC-NTC controller, the temperature constraint is temporarily violated during 1.49 s with a maximal peak of 405.1 K. On the other hand, the MPC-QP and MPC-SDP controllers keep the temperature profile below 400 K along the test. Regarding the control actions of the control systems, they were all the time within the allowed limits.

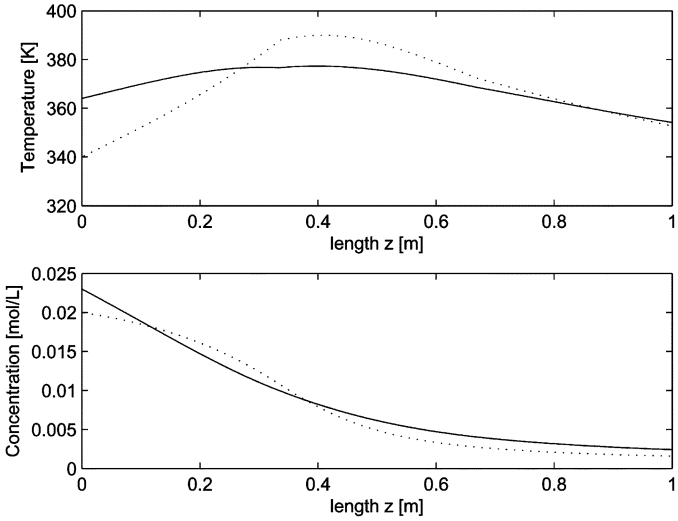

Fig. 6. Steady-state temperature and concentration profiles for Test 3. Dotted line—reference. Solid line—MPC-QP. Dashed line—MPC-SDP. Dashdot line—MPC-NTC.

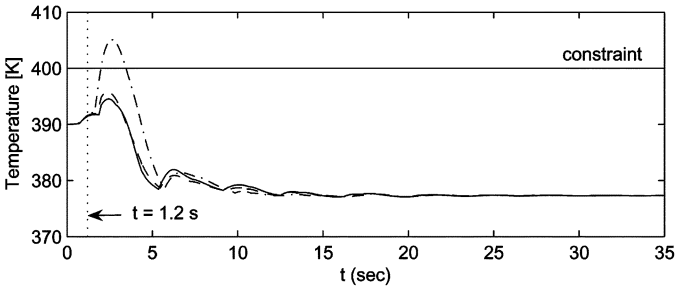

Fig. 7. Maximal peak of the temperature profile during Test 3. Solid Line—MPC-QP. Dashed line—MPC-SDP. Dashdot line—MPC-NTC.

Fig. 8 shows the cost function values obtained with the MPC-QP and MPC-SDP controllers along Test 3. We can see that the largest differences occur between $t = 1$ s and $t = 5.6$ s approximately. Notice that along this interval the temperature constraints are active and the differences in the cost function values are due to the polynomial approximation of these constraints. After this interval the difference between the cost function values becomes small and at the end practically negligible. The predictions of the temperature profile at $t = 1.2$ s of the MPC-QP and MPC-SDP controllers are plotted in Figs. 9 and 10, respectively. The maximal peak of these predictions can be found by projecting the plots shown in Figs. 9 and 10 on the plane $z = 0$. Fig. 11 shows the controllers' predictions of the maximal peak of the temperature profile at $t = 1.2$ s. From Fig. 11 it is clear that the temperature constraints of MPC-QP and MPC-SDP are active. Both controllers keep the temperature below and on 400 K along the prediction horizon. The differences observed between the predictions of MPC-QP and MPC-SDP, are mainly due to the errors of approximating the temperature constraints with polynomials. If we want to reduce

Authorized licensed use limited to: Katholieke Universiteit Leuven. Downloaded on September 1, 2009 at 08:41 from IEEE Xplore. Restrictions apply.

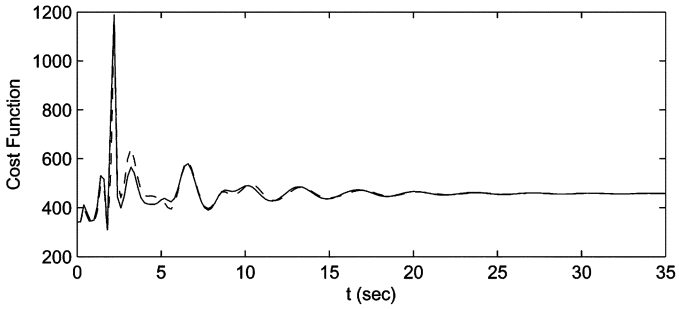

Fig. 8. Cost function values during Test 3. Solid Line—MPC-QP. Dashed line—MPC-SDP.

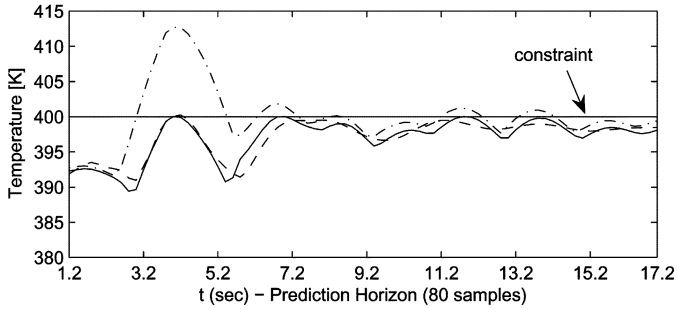

Fig. 11. Predictions of the maximal peak of the temperature profile at $t = 1.2$ s (Test 3). Solid Line—MPC-QP. Dashed line—MPC-SDP. Dashdot line—MPC-NTC.

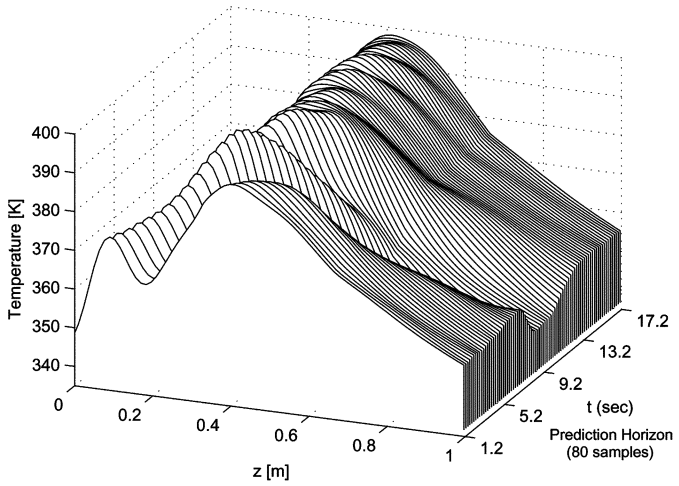

Fig. 9. MPC-QP predictions of the temperature profile at $t = 1.2$ s (Test 3).

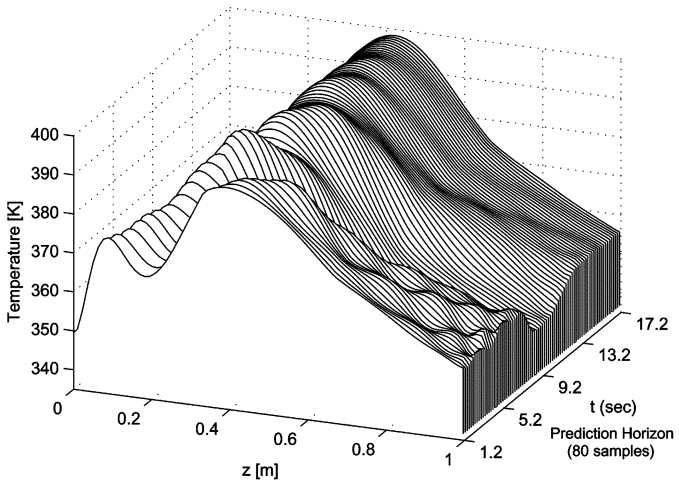

Fig. 10. MPC-SDP predictions of the temperature profile at $t = 1.2$ s (Test 3).

these discrepancies, we would have to increase the degree of the polynomials. However, this would lead to an increment in the number of constraints and optimization variables which would increase the complexity of the optimization problem and therefore the time required to solve it. Additionally, tests with larger polynomial degrees would cause numerical instabilities within *Sedumi*.

Notice that in Test 3, the closed-loop response of the controlled system is different than the predicted one. Also observe that the steady state profiles of the reactor are far from the desired ones. None of these situations occurred during Tests 1 and 2. All of this is mainly due to considerable differences between the linear POD model used by the controllers and the observer, and the nonlinear model of the process. We have to keep in mind that during Test 3 the reactor is operating far away from the profiles (see Fig. 2) where the nonlinear model of the reactor was linearized. It is quite clear that we have to incorporate the nonlinearities of the process into the POD model used by the controllers if we want to improve the performance of the control systems. Nevertheless this would lead to non-convex optimization problems that would require more advanced solvers. For instance, the optimization problems of the nonlinear MPC-QP and MPC-SDP controllers could be addressed by Sequential Quadratic Programming (SQP) and sequential SDP methods, respectively.

Table I presents the average computation times (in a PC with a Dual Core of 3 Ghz and a RAM memory of 2 GB) for solving the optimization problems of the MPC controllers during Test 3 for different control and prediction horizons. In Table I, we also have included the time of solving the optimization of the MPC-QP controller when a specialized QP solver like *Quadprog* is used. *Quadprog* is part of the Optimization Toolbox of Matlab [34] and it uses an active set method similar to that described in [35]. From Table I it is clear that the optimization of the MPC-SDP controller requires less time than the optimization of the MPC-QP controller when we use the same solver (*Sedumi*) for both cases. However if we use *Quadprog* (in general it is more efficient to solve a QP problem using a QP solver like *Quadprog* than using a more general tool like *Sedumi*) for solving the optimization of the MPC-QP controller, the time required is between 14 to 19 times shorter than the time needed to solve the optimization of the MPC-SDP controller.

Table II shows the number of optimization variables (including auxiliary variables), the number and kind of constraints and the memory requirements of the predictive controllers. It is important to remark that the MPC-SDP controller has been encoded using explicitly the primal representation in *Sedumi* whereas the MPC-QP (*Sedumi*) controller has been implemented using the dual formulation. Therefore the values in Table II for these controllers correspond to the number of optimization variables and constraints in the primal (MPC-SDP) and dual space (MPC-QP) respectively. Notice that for the MPC-SDP case, the LMI constraints introduce a large number

Authorized licensed use limited to: Katholieke Universiteit Leuven. Downloaded on September 1, 2009 at 08:41 from IEEE Xplore. Restrictions apply.

TABLE I
AVERAGE TIME FOR SOLVING THE OPTIMIZATION PROBLEM

Control	$N_c = 5$ $N_p = 75$	$N_c = 10$ $N_p = 80$	$N_c = 15$ $N_p = 85$	$N_c = 20$ $N_p = 90$
MPC-QP (*Sedumi*)	6.74 s	13.01 s	21.33 s	32.89 s
MPC-QP (*Quadprog*)	0.28 s	0.31 s	0.53 s	0.76 s
MPC-SDP	3.91 s	5.77 s	8.09 s	11.2 s

Note: N_c and N_p are the control and prediction horizons in samples.

TABLE II
NUMBER OF VARIABLES, NUMBER OF CONSTRAINTS AND MEMORY REQUIREMENTS WHEN $N_c = 10$ AND $N_p = 80$

Control	No. Opt. Variables	Number of Constraints				Memory (MB)
		Ineq.[a]	Equ.[b]	SOC[c]	LMI[d]	
MPC-QP (*Sedumi*)	32	24061	-	1	-	6.2
MPC-QP (*Quadprog*)	31	24061	-	-	-	6.02
MPC-SDP	7378	61	2065	2	80	0.67

[a]Inequality constraints.
[b]Equality constraints.
[c]Second Order Cone constraints.
[d]Linear Matrix Inequality constraints.

of variables. This is the main drawback of our approach. However in spite of this, the optimization problem for the MPC-SDP case requires less time than the case when *Sedumi* is used to solve the optimization of the MPC-QP controller. Nevertheless If we keep increasing the degree of the polynomials used to approximate the temperature constraints, we will reach a point where the time required for solving the optimization of the MPC-SDP controller would be larger than the time needed to solve the optimization of MPC-QP with *Sedumi*.

Finally, from Table II we can see that the memory requirements (the memory needed to store the matrices that are given to the solver) of the MPC-SDP controller are significantly less than the memory requisites of the MPC-QP controller (it does not matter the solver used). The MPC-SDP controller requires approximately 9 times less memory than the MPC-QP controller. Although our approach has not led to a reduction in the computational time (when the optimization of MPC-QP is performed with *Quadprog*), it certainly has led to a remarkable saving of memory.

VII. CONCLUSION

In this paper, a method for approximating the temperature constraints of a POD-based predictive controller for a tubular reactor has been presented. In this method, part of the basis vectors derived with the POD technique are approximated with univariate real polynomials. Afterwards, the theory of positive polynomials is used for approximating the temperature constraints by means of LMIs and linear equality constraints. The method leads to a significant reduction in the number of constraints which conduces to a considerable saving of the memory. However the computational time needed for solving the optimization problem of the predictive controller based on the polynomial approximations, is much larger than the time required for solving the original problem. What mainly limits the computational gain of this technique is the large number of variables that are introduced by the LMI constraints. From this study it is clear that with this positive polynomial approach the resulting optimization problem is more complex than the original one. Nevertheless our approach guarantees the fulfillment of the temperature constraint at every point of the reactor. Other ways of tackling the problem are also possible and might be efficient. Future work is necessary in order to find out which approach works best for which kind of applications.

The predictive controller based on the polynomial approximation presented a good behavior, and it was able to deal with the temperature constraints quite well.

An interesting topic for further investigation concerns robustness considerations with respect to model uncertainties. Notice that at the moment of incorporating these uncertainties, we need to preserve the LMI representation of our model. This excludes the use of multivariate polynomials, which are not exactly representable as LMIs. However, there is still some breathing space for robust approaches in our setting. Robustness of semidefinite optimization problems has been studied by Ben Tal, El Ghaoui, and Nemirovski in [36]. They show that robust semidefinite optimization, while NP-hard even in simple uncertainty settings, can be approximated by a semidefinite relaxation. It is also possible to obtain some accuracy bounds for some of these relaxations, namely when they use an ellipsoidal uncertainty on the coefficient of the affine constraints. In particular, we can apply their theory if we consider that the coefficients of the interpolation theorems are only known within some prescribed accuracy. Our approach, that we only applied to linear system models so far, can in a straightforward way be generalized to the case of nonlinear MPC and would then lead to the interesting problem class of nonlinear SDP problems that can e.g., be addressed by the sequential SDP methods proposed and investigated in [37]–[39].

ACKNOWLEDGMENT

The authors would like to thank the reviewers of this manuscript for their suggestions and remarks that undoubtedly contributed to the improvement of our initial submission.

REFERENCES

[1] M. Hazenberg, P. Astrid, and S. Weiland, "Low order modeling and optimal control design of a heated plate," in *Proc. 5th Eur. Control Conf.*, Cambridge, U.K., Sep. 2003, [CD ROM].
[2] O. M. Agudelo, J. J. Espinosa, and B. De Moor, "Control of a tubular chemical reactor by means of POD and predictive control techniques," in *Proc. Eur. Control Conf. (ECC'07)*, Kos, Greece, Jul. 2007, pp. 1046–1053.
[3] M. Hovd and R. D. Braatz, "Handling state and output constraints in MPC using time-dependent weights," in *Proc. Amer. Control Conf. (ACC)*, Arlington, VA, 2001, pp. 2418–2423.
[4] I. Y. Smets and J. F. Van Impe, "Optimal control of tubular chemical reactors: Performance assessment under transient and diffuse conditions," in *Proc. 10th Med. Conf. Control Automat. (MED'02)*, Lisbon, Portugal, 2002, [CD ROM].
[5] M. Fjeld and B. Ursin, "Approximate lumped models of a tubular chemical reactor, and their use in feedback and feedforward control," in *Proc. 2nd IFAC Symp. Multivariable Technical Control Syst.*, Amsterdam, The Netherlands, 1971, pp. 1–18.
[6] P. Astrid, "Reduction of Process Simulation Models: A Proper Orthogonal Decomposition Approach," Ph.D. dissertation, Technishche Universiteit Eindhoven, Eindhoven, The Netherlands, 2004.

Authorized licensed use limited to: Katholieke Universiteit Leuven. Downloaded on September 1, 2009 at 08:41 from IEEE Xplore. Restrictions apply.

[7] A. Chatterjee, "An introduction to the proper orthogonal decomposition," *Current Sci.*, vol. 78, no. 7, pp. 808–817, Apr. 2000.
[8] Y. C. Liang, H. P. Lee, S. P. Lim, W. Z. Lin, K. H. Lee, and C. G. Wu, "Proper orthogonal decomposition and its applications-Part I: theory," *J. Sound Vibration*, vol. 252, no. 3, pp. 527–544, May 2002.
[9] S. Chakravarti, M. Marek, and W. H. Ray, "Reaction-diffusion system with brusselator kinetics: Control of a quasiperiodic route to chaos," *Phys. Rev. E*, vol. 52, no. 3, pp. 2407–2423, Sep. 1995.
[10] J. Lumley and P. Blossey, "Control of turbulence," *Annu. Rev. Fluid Mech.*, vol. 30, pp. 311–327, 1998.
[11] A. Theodoropoulou, R. A. Adomaitis, and E. Zafiriou, "Model reduction for optimization of rapid thermal chemical vapor deposition systems," *IEEE Trans. Semicond. Manufact.*, vol. 11, pp. 85–98, Feb. 1998.
[12] W. R. Graham, J. Peraire, and K. Y. Tang, "Optimal control of vortex shedding using low-order models. Part I-open-loop model development," *Int. J. Numer. Methods Eng.*, vol. 44, no. 7, pp. 945–972, 1999.
[13] E. A. Gillies, "Low-dimensional control of the circular cylinder wake," *J. Fluid Mech.*, vol. 371, pp. 157–178, 1998.
[14] K. Kunisch and S. Volkwein, "Control of the burgers equation by a reduced-order approach using proper orthogonal decomposition," *J. Optim. Theory Appl.*, vol. 102, no. 2, pp. 345–371, Aug. 1999.
[15] S. S. Ravindran, "A reduced-order approach for optimal control of fluids using proper orthogonal decomposition," *Int. J. Numer. Methods Fluids*, vol. 34, no. 5, pp. 425–448, Nov. 2000.
[16] P. Beyer, S. Benkadda, and X. Garbet, "Proper orthogonal decomposition and Galerkin projection for a three-dimensional plasma dynamical system," *Phys. Rev. E*, vol. 61, no. 1, pp. 813–823, Jan. 2000.
[17] A. K. Bangia, P. F. Batcho, I. G. Kevrekidis, and G. E. Karniadakis, "Unsteady two-dimensional flows in complex geometries: Comparative bifurcation studies with global eigenfunction expansions," *SIAM J. Sci. Comput.*, vol. 18, no. 3, pp. 775–805, 1997.
[18] A. Liakopoulos, P. A. Blythe, and H. Gunes, "A reduced dynamical model of convective flows in tall laterally heated cavities," *Proc. Royal Soc. A: Math., Phys. Eng. Sci.*, vol. 453, no. 1958, pp. 663–672, 1997.
[19] A. Iollo, S. Lanteri, and J. A. Désidéri, "Stability properties of POD-Galerkin approximations for the compressible Navier-stokes equations," *Theor. Computat. Fluid Dyn.*, vol. 13, no. 6, pp. 377–396, Mar. 2000.
[20] L. Huisman, "Control of Glass Melting Processes Based on Reduced CFD Models," Ph.D. dissertation, Technishche Universiteit Eindhoven, Eindhoven, The Netherlands, 2005.
[21] L. Huisman and S. Weiland, "Reduced model based LQG control of an industrial glass feeder," in *Proc. 10th IFAC/IFORS/IMACS/IFIP Symp. Large Scale Syst.: Theory Appl.*, Osaka, Japan, Jul. 2004, vol. 1, pp. 421–426.
[22] L. Huisman and S. Weiland, "Identification and model predictive control of an industrial glass feeder," in *Proc. 13th IFAC Symp. Syst. Identification (SYSID'03)*, Rotterdam, The Netherlands, Aug. 2003, pp. 1685–1689.
[23] P. Holmes, Lumley, and G. Berkooz*, Turbulence, Coherence Structure, Dynamical Systems and Symmetry*. Cambridge, U.K.: Cambridge University Press, 1996.
[24] T. W. Parks and C. S. Burrus*, Digital Filter Design*. New York: Wiley, 1987.
[25] M. Hovd and R. D. Braatz, "On the use of soft constraints in MPC controllers for plants with inverse response," in *Proc. 6th IFAC Symp. Dyn. Control Process Syst.*, Jejudo, Korea, 2001, pp. 251–256.
[26] P. O. M. Scokaert and J. B. Rawlings, "Feasibility issues in linear model predictive control," *AIChE J.*, vol. 45, pp. 1649–1659, 1999.
[27] B. Pluymers, J. A. K. Suykens, and B. D. Moor, Construction of Reduced Complexity Polyhedral Invariant Sets for LPV Systems Using Linear Programming ESAT-SISTA, K.U. Leuven, Leuven, Belgium, Tech. Rep. 05-172, 2005.
[28] Y. Nesterov, "Squared functional systems and optimization problems," in *High Performance Optimization*, H. Frenk, K. Roos, T. Terlaky, and S. Zhang, Eds. New York: Kluwer, 2000, pp. 405–440.
[29] P. A. Parrilo, "Structured Semidefinite Programs and Semialgebraic Geometry Methods in Robustness and Optimization," Ph.D. dissertation, California Institute of Technology, Pasadena, 2000.
[30] A. Ben-Tal and A. Nemirovski*, Lectures on Modern Convex Optimization: Analysis, Algorithms, and Engineering Applications*, ser. MPS/SIAM Series on Optimization. Philadelphia, PA: SIAM, 2001.
[31] Y. Nesterov and M. Todd, "Self-scaled barriers and interior-point methods for convex programming," *Math. Operat. Res.*, vol. 22, pp. 1–42, 1997.
[32] J. Sturm, "Using SeDuMi 1.02, a MATLAB toolbox for optimization over symmetric cones," *Optim. Methods Software*, vol. 11, pp. 625–653, 1999.
[33] D. D. Vecchio and N. Petit, "Boundary control for an industrial underactuated tubular chemical reactor," *J. Process Control*, vol. 15, pp. 771–784, 2005.
[34] *"Optimization Toolbox 3: User's Guide,"* Mathworks, 2006.
[35] P. E. Gill, W. Murray, and M. H. Wright*, Practical Optimization*. London, U.K.: Academic, 1981.
[36] A. Ben-Tal, L. G. El, and A. Nemirovski, "Robustness," in *Handbook of Semidefinite Programming*, H. Wolkowicz, R. Saigal, and L. Venberghe, Eds. New York: Kluwer, 2000, pp. 139–162.
[37] B. Fares, D. Noll, and P. Apkarian, "Robust control via sequential semidefinite programming," *SIAM J. Control Optim.*, vol. 40, no. 6, pp. 1791–1820, 2002.
[38] R. W. Freund and F. Jarre, A Sensitivity Analysis and a Convergence Result for a Sequential Semidefinite Programming Method Bell Laboratories, Murray Hill, NJ, Tech. Rep., 2003.
[39] M. Diehl, F. Jarre, and C. Vogelbusch, "Loss of superlinear convergence for an SQP-type method with conic constraints," *SIAM J. Optim.*, vol. 16, no. 4, pp. 1201–1210, 2006.



Oscar Mauricio Agudelo received the B.S. degree in electronics engineering from the Universidad Autónoma de Occidente, Cali, Colombia, in 1997, the M.S. degree in Industrial Control engineering from the Universidad de Ibagué (in cooperation with Katholieke Universiteit Leuven and Universiteit Gent), Ibagué, Colombia, in 2004, and is currently pursuing the Ph.D. degree at the Department of Electrical Engineering (ESAT), Katholieke Universiteit Leuven, Leuven, Belgium.

From 1997 to 2004, he worked at the Universidad Autónoma de Occidente as a full time teacher of control and automation. His research interests are in model reduction techniques, proper orthogonal decomposition (POD), model predictive control, control of tubular chemical reactors, and analysis and design of intelligent control systems.



Michel Baes received the M.S. degree in applied mathematics engineering and the Ph.D. degree from the Catholic University of Louvain-la-Neuve, Belgium, in 2002 and 2006, respectively.

He is a Postdoctoral Fellow of the Optimization in Engineering Center (OPTEC), Katholieke Universiteit Leuven, Leuven, Belgium. His scientific interests include convex optimization and its applications, development of algebraic techniques dedicated to the design and the study of optimization algorithms.



Jairo José Espinosa (SM'06) received the B.S. degree in electronics engineering from the Universidad Distrital de Bogotá and the M.S. (with honors) and Ph.D. (with high honors) degrees in electrical engineering from the Katholieke Universiteit Leuven, Leuven, Belgium.

Currently, he is an Associate Professor with the National University of Colombia, Medellín. For many years he was R & D Manager for the company IPCOS N.V., Belgium, where he made research in advanced process control systems. He has been involved in the creation of products to construct inferential sensors, nonlinear model based predictive controllers and process optimization. He has hands on experience in many industrial areas including oil, polymers, petrochemicals, automotive, power generation and iron production where he has applied many of his developments. His research interests are intelligent control, nonlinear modeling, model based predictive control, inferential sensors, and model reduction techniques.

Authorized licensed use limited to: Katholieke Universiteit Leuven. Downloaded on September 1, 2009 at 08:41 from IEEE Xplore. Restrictions apply.



Moritz Diehl received the Ph.D. degree from the Interdisciplinary Center for Scientific Computing (IWR), Heidelberg University, Heidelberg, Germany, in 2001.

Since 2006, he has been a Professor with the University of Leuven (K.U. Leuven), Belgium, and principal investigator of K.U. Leuven's Optimization in Engineering Center OPTEC. His research is centered around embedded optimization algorithms for use in model predictive control, real-time optimization, and moving horizon estimation. His general interests are in structure exploitation for optimization in engineering, convex optimization, dynamic optimization. He works on real-world applications of optimization and control in mechatronics, robotics, sustainable energy, and chemical engineering.



Bart De Moor (SM'93–F'04) received the M.S. and Ph.D.degrees from the Katholieke Universiteit Leuven, Leuven, Belgium (KU. Leuven), in 1983 and 1988, respectively, both in electrical engineering.

He is a Full Professor with KU Leuven. He was a Visiting Research Associate at Stanford University, Stanford, CA, from 1988 to 1990. From 1991 to 1999, he was the chief advisor on science and technology for the Belgian Federal and the Flanders Regional Governments. He has published more than 250 journal papers, 350 conference proceedings publications, five books, and numerous science popularizing contributions. His research interests are in numerical linear algebra and optimization, system theory, control and identification, quantum information theory, datamining, information retrieval and bio-informatics.

Dr. De Moor received the Leybold-Heraeus Prize (1986), Leslie Fox Prize (1989), Guillemin-Cauer Best Paper Award of the *IEEE Transactions on Circuits and Systems* (1990), Laureate of the Belgian Royal Academy of Sciences (1992), bi-annual Siemens Award (1994), Best Paper Award of *Automatica* (IFAC, 1996), and the IEEE Signal Processing Society Best Paper Award (1999).

Authorized licensed use limited to: Katholieke Universiteit Leuven. Downloaded on September 1, 2009 at 08:41 from IEEE Xplore. Restrictions apply.